

Accurately computing weak lensing convergence

Sofie Marie Koksbang¹ and Chris Clarkson^{2,3,4}

¹University of Helsinki, Department of Physics and Helsinki Institute of Physics,
P.O. Box 64, FIN-00014 University of Helsinki, Finland*

²School of Physics & Astronomy, Queen Mary University of London, UK

³Department of Physics & Astronomy, University of the Western Cape, Cape Town 7535, South Africa

⁴Department of Mathematics and Applied Mathematics,
University of Cape Town, Rondebosch 7701, South Africa†

Weak lensing will play an important role in future cosmological surveys, including e.g. Euclid and the Square Kilometre Array. Sufficiently accurate theoretical predictions are important for correctly interpreting these surveys and hence for extracting correct cosmological parameter estimations. We quantify for the first time in a relativistic setting how many post-Born and lens-lens coupling corrections are required for sub-percent accuracy of the theoretical weak lensing convergence and distance-redshift relation for $z \leq 2$ (the primary weak lensing range for Euclid and SKA). We do this by randomly ray-tracing through a fully relativistic exact solution of the Einstein Field Equations which consists of randomly packed mass-compensated under-densities of realistic amplitudes. We find that one needs to include lens-lens coupling terms and post-Born corrections at least up to second and third order respectively for sub-percent accuracy of the convergence and angular diameter distance d_A . We find that, out of the random lines of sight studied, post-Born corrections can be as large as 70% of the total correction to the area distance. We also provide a simplified operator formalism for calculating the leading corrections to these quantities to arbitrary order.

Introduction

The linear expression for the convergence is well known and full second order expressions for the convergence are given in e.g. [1–5]. Third order corrections have only been considered partially, e.g. in [6]. Here, we focus on identifying the first, second and third order terms necessary to achieve perturbative results deviating less than $\sim 1\%$ from the exact convergence, κ , and angular diameter distance, d_A , up to a redshift of 2. This turns out to include lens-lens coupling at second order and post-Born corrections at second and third order. These we derive following procedures similar to those of [6]. We consider the shear contribution when computing d_A , but as the shear enters into the distance squared, we find it only needs to be considered at first-order. For sub-percent accuracy of the shear itself, higher order corrections are needed but as the shear can be approximately obtained from the convergence (see e.g. [7]) we do not investigate the necessary higher order corrections to the shear here, though we do provide a neat way to calculate them.

In order to compare the approximate κ and d_A obtained from perturbation theory, we study these quantities in exact Swiss-cheese models based on Lemaitre-Tolman-Bondi (LTB) structures describing mass compensated under-densities modelling voids arranged randomly in a Λ CDM background. Each LTB structure has a present time void with minimum $\delta\rho/\rho \approx 0.3$ and a radius ~ 30 Mpc and a compensating shell of over-density with $\delta\rho/\rho \sim 100$. Since the structures are randomly arranged and closely packed, the models give a good testing environment where the exact κ and d_A can be computed while sampling a large variety of lines of sight. The exact κ and d_A along light rays in the Swiss-cheese

model are compared with the perturbative approximations obtained from mock N-body reproductions of the Swiss-cheese models following the mapping procedure of [8, 9]. Within that setting, light rays can be traced using standard perturbation theory on a flat FLRW background combined with the non-linear density and velocity fields of the mock N-body data. The convergence, shear and angular diameter distance can then be computed using the equations derived below. The results are compared with the exact quantities which are obtained from the Sachs equations in the exact LTB spacetimes of the Swiss-cheese models.

Light propagation

The starting point for gravitational lensing is the geodesic deviation equation for a deviation vector ξ^a which separates neighboring null geodesics on a future pointing bundle k^a : $\ddot{\xi}^a + k^b \xi^c k^d R^a_{bcd} = 0$. We use R^a_{bcd} to denote the Riemann tensor, and dots indicate derivatives with respect to the affine parameter λ associated with k^a . Given an observer, the equation can be projected into a 2d screen space spanned by an orthonormal tetrad basis e^A_a , $A = 1, 2$. The equation then becomes $\ddot{\xi}_A = \mathcal{R}_{AB} \xi^B$, where the optical tidal matrix is given by $\mathcal{R}_{AB} = -\frac{1}{2} \delta_{AB} R_{cd} k^c k^d - C_{AcBd} k^c k^d$, with R_{ab} the Ricci tensor and C^a_{bcd} the Weyl tensor. Solutions are written in terms of the Jacobi map, \mathcal{J}_{AB} , as $\xi_A(\lambda) = \mathcal{J}_{AB}(\lambda) \zeta^B$ where \mathcal{J}_{AB} satisfies $\ddot{\mathcal{J}}_{AB} = \mathcal{R}_{AC} \mathcal{J}^C_B$, with $\mathcal{J}_{AB}(\lambda_o) = 0$ and $\dot{\mathcal{J}}_{AB}(\lambda_o) = -\delta_{AB}$. The differential equation can also be written as an integral equation which in matrix notation becomes $\mathcal{J} = (\lambda_o - \lambda_s) \mathcal{I} + \int_{\lambda_o}^{\lambda_s} d\lambda (\lambda_s - \lambda) \mathcal{R} \cdot \mathcal{J}$. The Jacobi map takes the observed angle between two rays at the observer, $\zeta^A := -\dot{\xi}^A|_o$, and maps it to the deviation vector at the source. The map can be expanded in terms of a background distance \bar{d}_A and an amplification matrix

$$\mathcal{A}_{AB} = (1 - \kappa)\delta_{AB} + \gamma_{AB} \text{ or}$$

$$\mathcal{J} = \bar{d}_A \mathcal{A} = \bar{d}_A \begin{pmatrix} 1 - \kappa - \gamma_1 & -\gamma_2 + \omega \\ -\gamma_2 - \omega & 1 - \kappa + \gamma_1 \end{pmatrix}. \quad (1)$$

The convergence is therefore $\kappa = 1 - \text{tr } \mathcal{J}/2\bar{d}_A$, and the shear is the trace-free part of \mathcal{A} . The angular diameter distance as a function of affine parameter is $d_A = \sqrt{\det \mathcal{J}} = \bar{d}_A \sqrt{(1 - \kappa)^2 - \gamma^2 + \omega^2}$, where a bar denotes background quantities and $\gamma^2 := \gamma_1^2 + \gamma_2^2$. The rotation ω does not affect the distance at any order we consider, so we ignore it from now on.

We shall now consider solving for the convergence perturbatively, assuming a weak field approximation. We consider a perturbed FLRW metric (using $c = 1 = 4\pi G$): $ds^2 = a^2 [- (1 + 2\Phi) d\eta^2 + (1 - 2\Psi) \gamma_{ij} dx^i dx^j]$, where $\gamma_{ij} = \delta_{ij}$ if x^i are Cartesian (i, j, k, \dots denote spatial indices). As only the sum of the potentials will appear we introduce the Weyl potential $\psi := (\Phi + \Psi)/2$. We will work on the conformal geometry, ignoring factors of a except where they appear in relation to $\delta\rho$. In this case the background angular diameter distance is $\bar{d}_A = r$, and we will use r as the affine parameter distance down the past light cone from observer to source: $r = \lambda_o - \lambda_s$. For this metric, the leading order perturbative contribution to the optical tidal matrix is

$$\delta\mathcal{R}_{AB} = -\delta_{AB}\delta\rho/a^2 - 2\nabla_{\langle A}\nabla_{B\rangle}\psi. \quad (2)$$

Note that we keep only the terms with the highest number of derivatives in screen space since these terms are by far the most important for normal lensing events. Angle brackets mean the trace-free part of a tensor: $X_{\langle AB\rangle} = X_{AB} - \frac{1}{2}\delta_{AB}\delta^{CD}X_{CD}$, and $\nabla^2 = \nabla_A \nabla^A$. (As we keep only highest derivatives of the potential, no derivatives of the tetrad appear.) If we identify ψ as the full gravitational potential (e.g., from an N-body simulation) rather than the potential from linear perturbation theory, this is an excellent approximation. We use the flat sky approximation so the derivatives in the above expression can simply be swapped with Cartesian derivatives in the final expressions. Note lastly that the Ricci term deviates from the exact Ricci term only in terms of Born corrections and Doppler corrections as the exact Ricci term is $-\frac{1}{2}\delta_{AB}R_{cd}k^c k^d \propto -\rho(k^\mu u_\mu)^2$.

Using $\delta\mathcal{R}$, the integral equation for the amplification matrix becomes

$$\mathcal{A} = \mathcal{I} + \int_0^r dr' \frac{r'(r - r')}{r} \delta\mathcal{R} \cdot \mathcal{A}. \quad (3)$$

Our goal is to solve this equation to obtain κ and d_A at sub-percent accuracy as will be necessary for the correct interpretation of and forecasts for upcoming surveys. We define the operator

$$\mathcal{O}_A^B(r, r') = - \int_0^r dr' \frac{r'(r - r')}{r} \delta\mathcal{R}_A^B(r'). \quad (4)$$

Repeated substitution then shows that the solution can be written as the series

$$\mathcal{A}_A^B(r) = \delta_A^B - \mathcal{O}_A^B(r, r') + \mathcal{O}_A^C(r, r')\mathcal{O}_C^B(r', r'') - \mathcal{O}_A^C(r, r')\mathcal{O}_C^D(r', r'')\mathcal{O}_D^B(r'', r''') + \dots. \quad (5)$$

The second term gives the standard linear convergence and shear:

$$\kappa(r) = \int_0^r dr' \frac{r'(r - r')}{r} a^2 \delta\rho(r'), \quad (6)$$

$$\gamma_{AB}(r) = 2 \int_0^r dr' \frac{r'(r - r')}{r} \nabla_{\langle A} \nabla_{B\rangle} \psi(r'), \quad (7)$$

with $-\gamma_{22} = \gamma_{11} = \gamma_1$, $\gamma_{12} = \gamma_{21} = -\gamma_2$.

Promoting these to operators, $\kappa(r) \rightarrow \kappa(r, r')$ and $\gamma_{AB}(r) \rightarrow \gamma_{AB}(r, r')$, we can separate the trace and trace-free parts of \mathcal{O}_{AB} as

$$\mathcal{O}_{AB}(r, r') = \kappa(r, r')\delta_{AB} + \gamma_{AB}(r, r'). \quad (8)$$

Using this we can now calculate the higher order contributions to the convergence and shear by extracting the trace and trace-free parts of the higher-order products of \mathcal{O}_{AB} . In general, a contraction of 2 symmetric matrix operators in 2d, $X_{AB} = X\delta_{AB} + \hat{X}_{AB}$, can be expanded into its trace and trace-free parts as

$$X_A^C Y_{CB} = \frac{1}{2}(2XY + \hat{X}^{CD}\hat{Y}_{CD})\delta_{AB} + X\hat{Y}_{AB} + \hat{X}_{AB}Y + \hat{X}_{\langle A}^C \hat{Y}_{B\rangle C}. \quad (9)$$

We can use this repeatedly to calculate all the higher-order contributions we require. Consequently we have the second-order convergence in terms of the first-order operators κ and γ_{AB} :

$$\begin{aligned} \kappa^{(2)}(r) &= \kappa_{\kappa\kappa} + \kappa_{\gamma\gamma} = -\kappa(r, r')\kappa(r', r'') - \frac{1}{2}\gamma^{AB}(r, r')\gamma_{AB}(r', r'') \\ &= - \int_0^r dr' \frac{r - r'}{r} a^2 \delta\rho(r') \int_0^{r'} dr'' (r' - r'') r'' a^2 \delta\rho(r'') \\ &\quad - 2 \int_0^r dr' \frac{r - r'}{r} \nabla^{\langle A} \nabla^{\rangle B} \psi(r') \times \int_0^{r'} dr'' (r' - r'') r'' \nabla_{\langle A} \nabla_{B\rangle} \psi(r''). \end{aligned} \quad (10)$$

Similarly we can read off the correction to the shear from the trace-free part as

$$\begin{aligned}\gamma_{AB}^{(2)} &= \kappa(r, r')\gamma_{AB}(r', r'') + \gamma_{AB}(r, r')\kappa(r', r'') + \gamma_{\langle A}^C(r, r')\gamma_{B\rangle C}(r', r'') \\ &= 4 \int_0^r dr' \frac{r - r'}{r} \nabla_{\langle A} \nabla^C \psi(r') \int_0^{r'} dr'' (r' - r'') r'' \nabla_{B\rangle} \nabla_C \psi(r'').\end{aligned}\quad (11)$$

For the third-order terms we now use $\mathcal{O}_A^C(r, r')\mathcal{O}_C^D(r', r'') = \kappa^{(2)}(r, r', r'')\delta_{AB} + \gamma_{AB}^{(2)}(r, r', r'')$, again promoting $\kappa^{(2)}$ and $\gamma_{AB}^{(2)}$ to operators and using (9):

$$\begin{aligned}\kappa^{(3)}(r) &= \kappa^{(2)}(r, r', r'')\kappa(r'', r''') + \frac{1}{2}\gamma_{AB}^{(2)}(r, r', r'')\gamma^{AB}(r'', r''') \\ &= -\kappa(r, r')\kappa(r', r'')\kappa(r'', r''') - \frac{1}{2}\gamma^{AB}(r, r')\gamma_{AB}(r', r'')\kappa(r'', r''') + \frac{1}{2}\kappa(r, r')\gamma_{AB}(r', r'')\gamma^{AB}(r'', r''') \\ &\quad + \frac{1}{2}\gamma_{AB}(r, r')\kappa(r', r'')\gamma^{AB}(r'', r''') + \frac{1}{2}\gamma_{\langle A}^C(r, r')\gamma_{B\rangle C}(r', r'')\gamma^{AB}(r'', r''')\end{aligned}\quad (12)$$

And so on. In this way we can see explicitly the different contributions to the higher-order convergence.

The second and third order lens-lens coupling correction, respectively, of the convergence and shear are not necessary for percent accuracy at $z < 2$ in the studied models but could be necessary at higher redshifts, and will be necessary for higher accuracy.

The integrals in these expressions are in principle to be taken along the real perturbed line of sight, but this makes them difficult to compute. Alternatively, we can simply interpret these integrals as being along the background light ray, an approximation known as the Born approximation. We can then obtain corrections to the Born approximation by expanding around the background line of sight as follows.

It follows from the geodesic equation that deviations, δx^A , to the light path in screen space are given by $\delta x^A = -2 \int_0^r dr'(r - r')\psi_{,A}(r')$. Different orders of δx^A

are obtained by Taylor expanding $\psi_{,A}$ around the unperturbed light path under the integral, while integrating according to the Born approximation, i.e. for the first and second order:

$$\begin{aligned}\delta x^{(1)A} &= -2 \int_0^r dr'(r - r')\psi_{,A}(r') \\ \delta x^{(2)A} &= -2 \int_0^r dr'(r - r')\psi_{,AB}(r')\delta x^{(1)B}(r') \\ &= 4 \int_0^r dr'(r - r')\psi_{,AB}(r') \int_0^{r'} dr''(r' - r'')\psi^{,B}(r'').\end{aligned}\quad (13)$$

Inserting these into the lowest perturbative expression for the amplification matrix gives the following corrections to the convergence:

$$\begin{aligned}\kappa_{B1} &= -2 \int_0^r dr' \frac{r - r'}{r} r' a^2 \delta \rho_{,A} \int_0^{r'} dr'' (r' - r'') \psi^{,A} \\ \kappa_{B2} &= 2 \int_0^r dr' \frac{r - r'}{r} r' a^2 \delta \rho_{,AB} \int_0^{r'} dr'' (r' - r'') \psi_{,A} \int_0^{r'} dr'' (r' - r'') \psi_{,B} \\ &\quad + 4 \int_0^r dr' \frac{r - r'}{r} r' a^2 \delta \rho_{,A} \int_0^{r'} dr'' (r' - r'') \psi_{,AB} \int_0^{r''} dr''' (r'' - r''') \psi_{,B}\end{aligned}\quad (14)$$

Lastly, it is necessary also to include the Doppler convergence κ_v in the computations (see e.g. [10]), which appears when we convert to redshift. The lowest order Doppler convergence is given by

$$\kappa_v = \left(1 - \frac{1}{ra_{,t}}\right) (\mathbf{v}_S - \mathbf{v}_O) \cdot \mathbf{n} + \mathbf{v}_O \cdot \mathbf{n}, \quad (15)$$

where \mathbf{n} is the direction vector of the light ray computed in the background and \mathbf{v}_S and \mathbf{v}_O are the spatial velocity fields of the source and observer, respectively. Provided \mathbf{v} is taken as the non-linear velocity, this formula is accurate enough.

Results We show the above discussed contributions

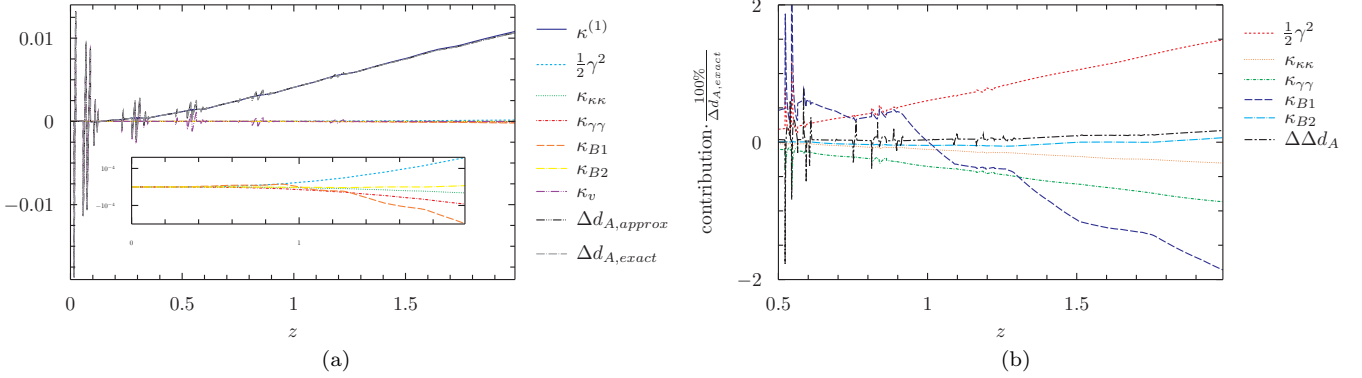


FIG. 1. Contributions to Δd_A along a fiducial light ray in the Swiss-cheese model. Left: Individual contributions including a close-up of the numerically smallest contributions. Right: Percentage of higher order contributions relative to the exact Δd_A . $\Delta\Delta d_A$ denotes the difference $\Delta d_{A,approximate} - \Delta d_{A,exact}$. The figure does not show the area with $z < 0.5$ as this area is obscured by peaks due to division by zero and mismatches of the exact and approximate Doppler convergences. The mismatches in the Doppler convergence will not be discussed here where cumulative effects along the light rays are the focus.

to the convergence and angular diameter distance along light rays propagated in Swiss-cheese models based on LTB structures specified by a Λ CDM background (the “cheese”) with $\Omega_\Lambda = 0.7$ and $H_0 = 70$ km/s/Mpc, a constant big bang time and a curvature parameter given by

$$k(r) = \begin{cases} -5.57 \cdot 10^{-8} r^2 \left(\left(\frac{r}{40 \text{Mpc}} \right)^6 - 1 \right)^6 & \text{if } r < 40 \text{Mpc} \\ 0 & \text{otherwise} \end{cases} \quad (16)$$

The LTB structures are arranged randomly in a periodic box of length 860Mpc by using the Jodrey-Torey algorithm [11, 12] as described in [13], leading to a Swiss-cheese universe of random close-packed LTB structures with a packing fraction of ~ 0.6 .

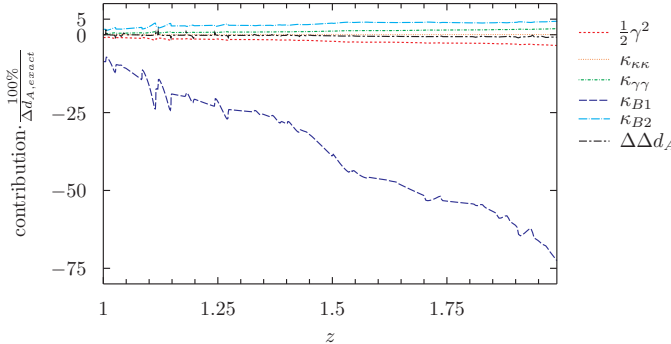


FIG. 2. Contributions to Δd_A along a random light ray with exceptionally large contribution from κ_{B1} in the high redshift. Only the higher part of the studied redshift interval is depicted as the lower parts is obscured by several divisions by zero.

Eleven random light rays have been considered, each with an observer in the Λ CDM background. By including the lowest order lens-lens coupling and the two lowest

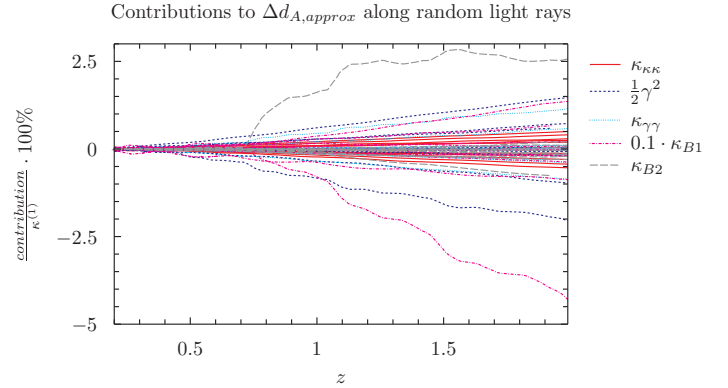


FIG. 3. Contributions to Δd_A along eleven random light rays in a Swiss-cheese model.

orders of post-Born corrections as well as the first order shear and $\kappa^{(1)} + \kappa_v$, the difference between the exact and approximate $\Delta d_A := \frac{\bar{d}_A - d_A}{\bar{d}_A}$ is less than 1% in the studied redshift interval when local effects from the Doppler convergence are ignored. An example is given in Fig. 1 which shows the individual contributions to Δd_A for one of the light rays. For this particular line of sight the second and third order contributions are all of similar size and most are $\sim 1\%$ or sub-percent individually while their sum is approximately 5% of $\Delta d_{A,exact}$. As indicated already in this figure, the lowest order post-Born correction is by far the most important contribution after $\kappa^{(1)} + \kappa_v$ and reaches the order of 10% along several of the studied light rays. As shown in Fig. 2 it reaches as much as 70% along one of the light rays. Naturally, it is along this light ray that also the third order post-Born correction is largest. It reaches approximately 4% at $z \approx 2$. The individual higher order corrections to the first order d_A along the eleven light rays are shown in figure 3 where they are shown relative to the standard

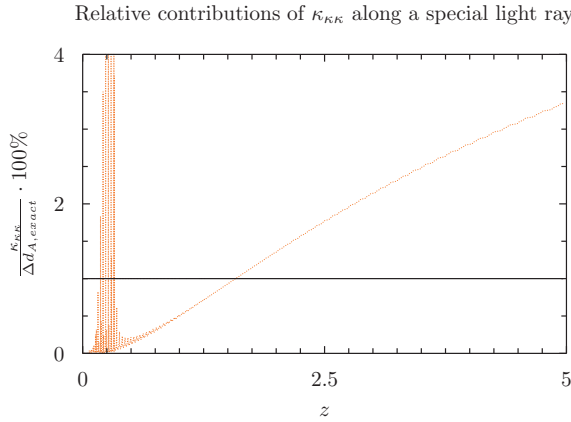


FIG. 4. Contribution of $\kappa_{\kappa\kappa}$ along a special light ray that passes radially through consecutive LTB structures. Peaks at low redshift are due to division by zero.

first order gravitational convergence $\kappa^{(1)}$. As seen, several contributions reach several percent of the size of $\kappa^{(1)}$ along a light ray. In fact, each of the higher order corrections reach 1% of both $\kappa^{(1)}$ and Δd_A individually along at least one of the studied light rays. The exception is $\kappa_{\kappa\kappa}$ which typically lies in the range $\sim 0.25\% - 0.75\%$ of Δd_A along the eleven random light rays and does not reach 1% along any of those rays. However, it reaches 1% at a redshift of $z \approx 1.5$ along the special light ray where LTB models are aligned so that the light ray passes radially through each structure. This is shown in figure 4. It is quite plausible that $\kappa_{\kappa\kappa}$ exceeds 1% along other less special light rays and is albeit close to 1% along several of the studied random rays.

Conclusion By comparing approximate weak lensing convergence and angular diameter distances with their exact counter parts we show that a sub-percent accuracy up to $z \approx 2$ of the angular diameter distance and weak lensing convergence requires several orders of the post-Born correction as well as the lowest order lens-lens coupling correction. Since most contributions to the convergence are in the form of integrals along the line of sight, even higher order corrections are needed if the same accuracy is required at higher redshifts. Our results thus show that the correct treatment of upcoming surveys will require the inclusion of several higher order corrections to the standard gravitational convergence $\kappa^{(1)}$. Our results also indicate that already for current surveys, including the post-Born correction at lowest order is important as it can become the dominant contribution to the convergence along some lines of sight. This point is worth further investigation, e.g., by using the method described here for computing the first order post-Born correction along light rays in N-body simulations. It would also be useful to use the method studied here for computing κ to evaluate the accuracy of the multiple-lens approximation often used for ray tracing through N-body simulations.

Acknowledgments We thank Thomas Tram and Jeppe Dakin for correspondence on FFTW3 and Giovanni Marozzi for correspondence on the work presented in [3].

SMK is supported by the Independent Research Fund Denmark under grant number 7027-00019B. CC was supported by STFC Consolidated Grant ST/P000592/1.

* sofie.koksbang@helsinki.fi

† chris.clarkson@qmul.ac.uk

- [1] Obinna Umeh et al.: Nonlinear relativistic corrections to cosmological distances, redshift and gravitational lensing magnification. I - Key results, *Class. Quantum Grav.* 31 202001 (2014), [arXiv:1207.2109v3](https://arxiv.org/abs/1207.2109v3) [astro-ph.CO]
- [2] Obinna Umeh et al.: Nonlinear relativistic corrections to cosmological distances, redshift and gravitational lensing magnification. II - Derivation, *Class. Quantum Grav.* 31 205001 (2014), [arXiv:1402.1933v2](https://arxiv.org/abs/1402.1933v2) [astro-ph.CO]
- [3] Giovanni Marozzi: The luminosity distance-redshift relation up to second order in the Poisson gauge with anisotropic stress, *Class.Quant.Grav.* 32 (2015) 045004, [arXiv:1406.1135v4](https://arxiv.org/abs/1406.1135v4) [astro-ph.CO]
- [4] Ido Ben-Dayan et al.: The second-order luminosity-redshift relation in a generic inhomogeneous cosmology, [10.1088/1475-7516/2012/11/045](https://doi.org/10.1088/1475-7516/2012/11/045) , [arXiv:1209.4326v2](https://arxiv.org/abs/1209.4326v2) [astro-ph.CO]
- [5] G. Fanizza et al.: An exact Jacobi map in the geodesic light-cone gauge, *JCAP* 11 (2013) 019, [arXiv:1308.4935v2](https://arxiv.org/abs/1308.4935v2) [astro-ph.CO]
- [6] Tilman Troster, Ludovic Van Waerbeke: Weak lensing corrections to tSZ-lensing cross correlation, *JCAP* 11 (2014) 008, [arXiv:1408.6284v2](https://arxiv.org/abs/1408.6284v2) [astro-ph.CO]
- [7] Martin Kilbinger: Cosmology with cosmic shear observations: a review, *Rep. Prog. Phys.* 78 (2015) 086901, [arXiv:1411.0115v2](https://arxiv.org/abs/1411.0115v2) [astro-ph.CO]
- [8] S. M. Koksbang, S. Hannestad: Methods for studying the accuracy of light propagation in N-body simulations, *Phys. Rev. D* 91, 043508 (2015) , [arXiv:1501.01413v3](https://arxiv.org/abs/1501.01413v3) [astro-ph.CO]
- [9] S. M. Koksbang, S. Hannestad: Studying the precision of ray tracing techniques with Szekeres models, *Phys. Rev. D* 92, 023532 (2015), [arXiv:1506.09127v3](https://arxiv.org/abs/1506.09127v3) [astro-ph.CO]
- [10] Krzysztof Bolejko et al.: Anti-lensing: the bright side of voids, *Phys. Rev. Lett.* 110, 021302 (2013), [arXiv:1209.3142v3](https://arxiv.org/abs/1209.3142v3) [astro-ph.CO]
- [11] W. S. Jodrey and E. M. Tory: Computer simulation of close random packing of equal spheres, *Phys. Rev. A* 32, 2347 (1985), <https://doi.org/10.1103/PhysRevA.32.2347> Erratum: *Phys. Rev. A* 34, 675 (1986)
- [12] W. S. Jodrey and E. M. Tory: Computer simulation of isotropic, homogeneous, dense random packing of equal spheres. *Powder Tech.*, 30:111118, 1981, [http://dx.doi.org/10.1016/0032-5910\(81\)80003-4](http://dx.doi.org/10.1016/0032-5910(81)80003-4)
- [13] S. M. Koksbang: Light propagation in Swiss cheese models of random close-packed Szekeres structures: Effects of anisotropy and comparisons with perturbative results, *Phys. Rev. D* 95, 063532 (2017), [arXiv:1703.03572v2](https://arxiv.org/abs/1703.03572v2) [astro-ph.CO]